

Production of like-sign W pairs via double parton scattering

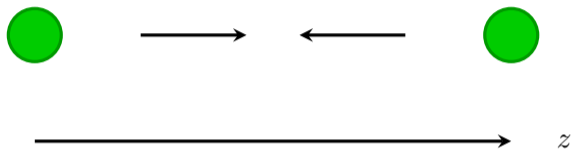
Oskar Grocholski
in collaboration with Markus Diehl

Seminar "Theory of Particle Physics and Cosmology"



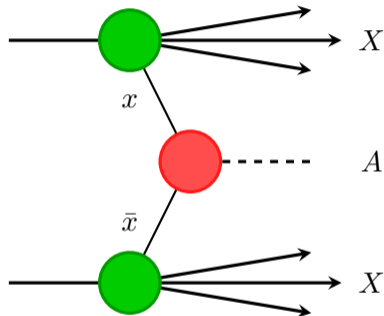
Warsaw, 9 May 2024

Single parton scattering



$$v^{\pm} = \frac{1}{\sqrt{2}}(v^0 \pm v^3)$$

Drell-Yan process: $pp' \longrightarrow A + X$



cross section = parton distribution functions \times parton-level cross section

Parton Distribution Function (PDF)

Definition of PDFs:

$$F_q(x; \mu) = \frac{1}{2} \int \frac{dz^-}{2\pi} e^{ixP^+z^-} \langle p | \bar{q}(-z/2) \Gamma q(z/2) | p \rangle \Big|_{z^+=|z|=0}. \quad (1)$$

$$\Gamma = \gamma^+, \gamma^5\gamma^+.$$

Double parton scattering

$$pp' \rightarrow A_1 + A_2 + X$$

A_i – produced in hard processes, X – summed over.

Hard scales: $Q_1, Q_2 \gg \Lambda$.

See: [M. Buffing, M. Diehl, T. Kasemets 2021 \[arXiv:1708.03528\]](#)

This work:

$$pp' \longrightarrow W^\pm W^\pm + X$$

Like-sign W pair production: SPS vs DPS

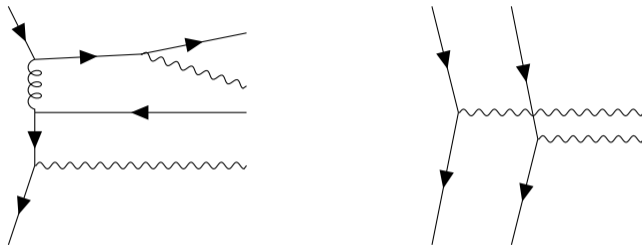


Figure: Single- (left) and double parton (right) Drell-Yan production of $W^\pm W^\pm$ pairs.

Like-sign W pair production: SPS vs DPS

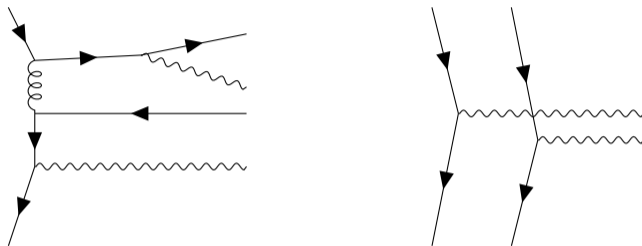


Figure: Single- (left) and double parton (right) Drell-Yan production of $W^\pm W^\pm$ pairs.

- $\sigma_{SPS} \propto \mathcal{O}(\alpha_S^2)$ with ≥ 2 jets.
- $\sigma_{DPS} \propto \mathcal{O}(\alpha_S^0)$,
- First observation of double parton scattering – [CMS, Phys.Rev.Lett. 131 \(2023\)](#).

Double parton factorization - an initial picture

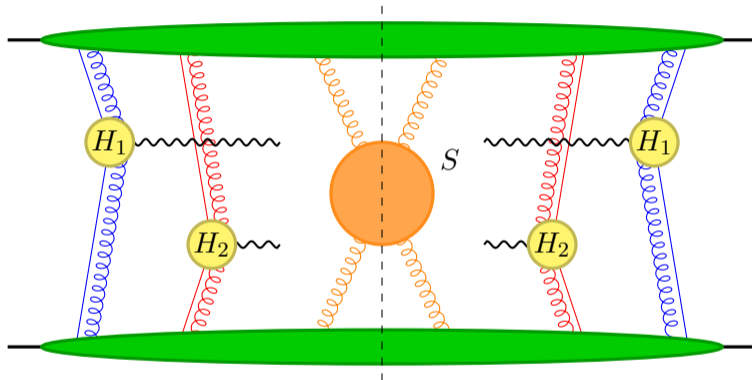
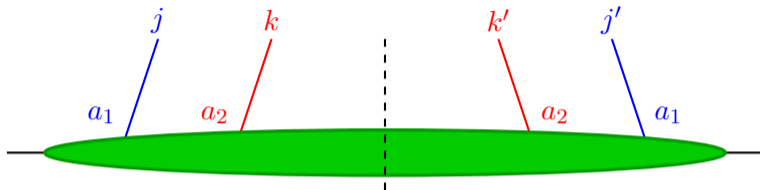


Figure: The general form of a leading-power graph representing the DPS.

Colour structure of DPDs

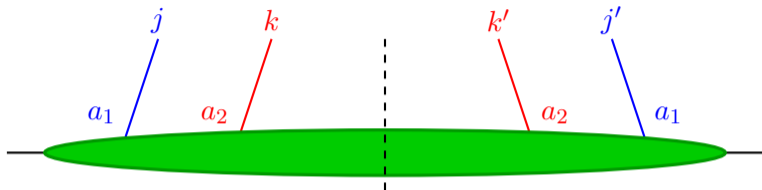


Parton carry colour indices \rightarrow project on SU(3) representations.

For quarks one can either project on $\delta_{jj'}\delta_{kk'}$ (colour singlet) or $t_{jj'}^c t_{kk'}^c$ (colour octet).

Gluons: $1, 8_S, 8_A, 10, \overline{10}, 27$.

Colour structure of DPDs



Parton carry colour indices \rightarrow project on SU(3) representations.

For quarks one can either project on $\delta_{jj'}\delta_{kk'}$ (colour singlet) or $t_{jj'}^c t_{kk'}^c$ (colour octet).

Gluons: $1, 8_S, 8_A, 10, \overline{10}, 27$.

Notation

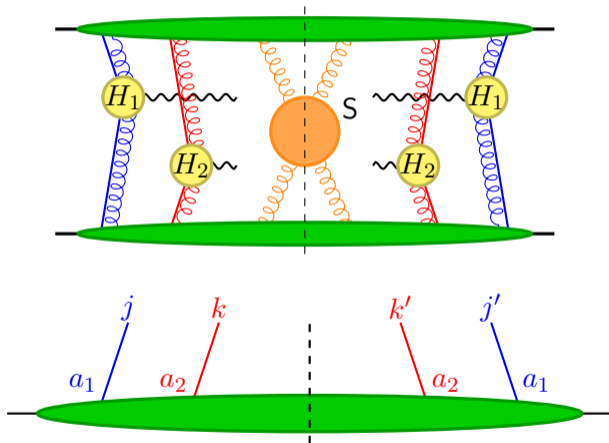
$R_1 R_2 F_{a_1 a_2}$ for parton a_i in representation R_i . $\dim(R_1) = \dim(R_2)$.

Evolution of DPDs

Roughly:

$\mu_1, \mu_2 \leftrightarrow$ cut-off on
virtuality of parton 1 and 2.
 \rightarrow Double DGLAP
evolution.

$\zeta \leftrightarrow$ cut-off on soft gluons
rapidities.
 \rightarrow Collins-Soper equation.



Double Drell-Yan production of $W^\pm W^\pm$

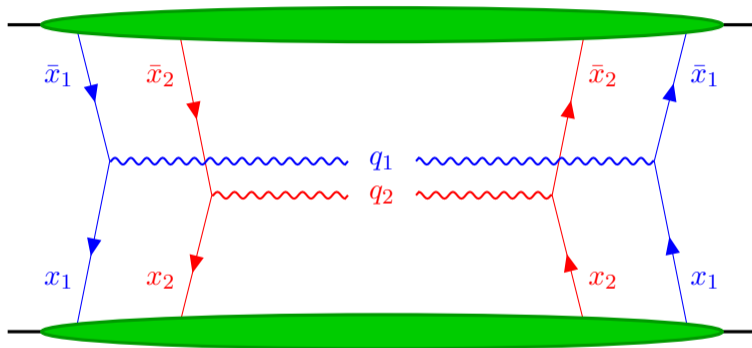
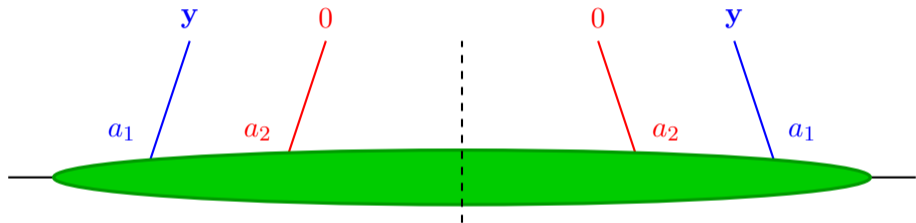


Figure: LO Feynman diagram representing the DPD contribution to $W^\pm W^\pm$ production.

Cross-section integrated over transverse momenta

$$\frac{d\sigma_{DPS}}{\prod_{i=1,2} dx_i d\bar{x}_i} = \frac{1}{1 + \delta_{A_1 A_2}} \sum_{a,b} \hat{\sigma}_{a_1 b_1 \rightarrow A_1} \hat{\sigma}_{a_2 b_2 \rightarrow A_2} \\ \times \int d^2 \mathbf{y} \sum_{R_i}^{R_1 R_2} F_{a_1 a_2}^{coll.}(x_i, \mathbf{y})^{\bar{R}_1 \bar{R}_2} F_{b_1 b_2}^{coll.}(\bar{x}_i, \mathbf{y}) . \quad (2)$$

Collinear DPDs

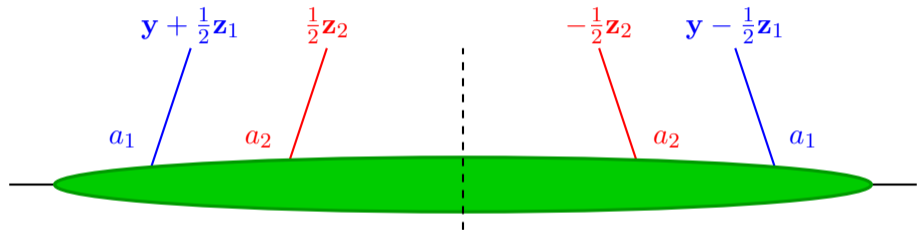


y – transverse distance between partons 1 and 2.

$$\begin{aligned}
 \frac{d\sigma_{DPS}}{\prod_{i=1,2} dx_i d\bar{x}_i d^2\mathbf{q}_i} &= \frac{1}{1 + \delta_{A_1 A_2}} \sum_{a,b} \hat{\sigma}_{a_1 b_1 \rightarrow A_1} \hat{\sigma}_{a_2 b_2 \rightarrow A_2} \\
 &\times \prod_{i=1,2} \int d^2\mathbf{k}_i d^2\bar{\mathbf{k}}_i \delta^{(2)}(\mathbf{q}_i - \mathbf{k}_i - \bar{\mathbf{k}}_i) \\
 &\times \int d^2\mathbf{y} \sum_{R_i}^{R_1 R_2} F_{a_1 a_2}(x_i, \mathbf{k}_i, \mathbf{y})^{\bar{R}_1 \bar{R}_2} F_{b_1 b_2}(\bar{x}_i, \bar{\mathbf{k}}_i, \mathbf{y}) . \quad (3)
 \end{aligned}$$

$$\begin{aligned} \frac{d\sigma_{DPS}}{\prod_{i=1,2} dx_i d\bar{x}_i d^2\mathbf{q}_i} &= \frac{1}{1 + \delta_{A_1 A_2}} \sum_{a,b} \hat{\sigma}_{a_1 b_1 \rightarrow A_1} \hat{\sigma}_{a_2 b_2 \rightarrow A_2} \\ &\times \prod_{i=1,2} \int \frac{d^2\mathbf{z}_i}{(2\pi)^2} e^{-i\mathbf{q}_i \mathbf{z}_i} \\ &\times \int d^2\mathbf{y} \sum_{R_i}^{R_1 R_2} F_{a_1 a_2}(x_i, \mathbf{z}_i, \mathbf{y})^{\bar{R}_1 \bar{R}_2} F_{b_1 b_2}(\bar{x}_i, \mathbf{z}_i, \mathbf{y}) . \end{aligned} \quad (4)$$

DTMD in the transverse position space



$y_{\pm} = y \pm \frac{1}{2}(z_1 - z_2)$ – distance between parton pairs on the left/right.

$$\begin{aligned} & \frac{d\sigma^{DPS}}{\prod_{i=1,2} dx_i d\bar{x}_i d^2\mathbf{q}_i} \\ & \propto \sum_{a_1, a_2, b_1, b_2} \hat{\sigma}_{a_1 b_1}(Q_1^2; \mu_1) \hat{\sigma}_{a_2 b_2}(Q_2^2; \mu_2) \\ & \times \int \frac{d^2\mathbf{z}_1}{(2\pi)^2} \frac{d^2\mathbf{z}_2}{(2\pi)^2} d^2\mathbf{y} e^{-i\mathbf{q}_1\mathbf{z}_1 - i\mathbf{q}_2\mathbf{z}_2} \\ & \times \sum_{R_i}^{R_1 R_2} F_{a_1 a_2}(x_i, \mathbf{z}_i, \mathbf{y})^{\bar{R}_1 \bar{R}_2} F_{b_1 b_2}(\bar{x}_i, \mathbf{z}_i, \mathbf{y}) \end{aligned}$$

$$\frac{d\sigma^{DPS}}{\prod_{i=1,2} dx_i d\bar{x}_i d^2\mathbf{q}_i}$$
$$\propto \sum_{a_1, a_2, b_1, b_2} \hat{\sigma}_{a_1 b_1}(Q_1^2; \mu_1) \hat{\sigma}_{a_2 b_2}(Q_2^2; \mu_2)$$
$$\times \int \frac{d^2\mathbf{z}_1}{(2\pi)^2} \frac{d^2\mathbf{z}_2}{(2\pi)^2} d^2\mathbf{y} \quad e^{-i\mathbf{q}_1\mathbf{z}_1 - i\mathbf{q}_2\mathbf{z}_2}$$
$$\times \sum_{R_i}^{R_1 R_2} F_{a_1 a_2}(x_i, \mathbf{z}_i, \mathbf{y})^{\bar{R}_1 \bar{R}_2} F_{b_1 b_2}(\bar{x}_i, \mathbf{z}_i, \mathbf{y})$$

$$\Lambda \ll |\mathbf{q}_i| \ll Q_i$$

Additional assumption about the scales:

$$\Lambda \ll |\mathbf{q}_i| \ll Q_i$$

\Rightarrow the most important contribution from the region of small \mathbf{z}_i :

$$|\mathbf{z}_i| \lesssim |\mathbf{q}_i|^{-1} \ll \Lambda^{-1}.$$

$$\Lambda \ll |\mathbf{q}_i| \ll Q_i$$

Additional assumption about the scales:

$$\Lambda \ll |\mathbf{q}_i| \ll Q_i$$

\implies the most important contribution from the region of small \mathbf{z}_i :

$$|\mathbf{z}_i| \lesssim |\mathbf{q}_i|^{-1} \ll \Lambda^{-1}.$$

We need to consider 2 sub-regions:

- $|\mathbf{y}| \sim |\mathbf{z}| \ll \Lambda^{-1}$: DTMD can be expressed in terms of PDFs (splitting) and twist-four distributions.
- $|\mathbf{y}| \gg |\mathbf{z}|$: use operator product expansion to match DTMDs onto collinear double parton distributions (DPDF).

Large \mathbf{y} approximation

Assume $|\mathbf{y}| \gg |\mathbf{z}_i|$.

Let us apply the operator product expansion to operators defining DTMDs:

$${}^R\mathcal{O}_a(x_i, \mathbf{y}, \mathbf{z}) = \sum_b \sum_{R'} {}^{R\bar{R}'} C_{ab}(x', \mathbf{z}) \otimes_x {}^{R'} \mathcal{O}_b(x', \mathbf{y}, \mathbf{z} = 0). \quad (5)$$

Matrix elements of a product of two $\mathcal{O}_b(x', \mathbf{y}, \mathbf{z} = 0)$ define collinear DPDFs.

Matching formula

$${}^{R_1 R_2} F_{a_1, a_2}(x, \bar{x}, \mathbf{y}, \mathbf{z}_i; \mu_{0i}, \zeta) = \sum_{b_1, b_2} \sum_{R'_1, R'_2} {}^{R_1 \bar{R}'_1} C_{a_1 b_1} \otimes_{x_1} {}^{R_2 \bar{R}'_2} C_{a_2 b_2} \otimes_{x_2} {}^{R'_1 R'_2} F_{b_1 b_2}^{coll.}(x'_i, \mathbf{y}; \mu_{0i}, \zeta), \quad (6)$$

with the kernels

$${}^{R_1 \bar{R}'_1} C_{a_1 b_1} = {}^{R_1 \bar{R}'_1} C_{a_1 b_1}(x_1, \mathbf{z}_1; \mu_{01}, x_1^2 \zeta), \quad (7)$$

known up to order α_S in both colour channels.

For reference see: [M. Buffing, M. Diehl, T. Kasemets 2021 \[arXiv:1708.03528\]](#)

Scales in the problem

- The natural choice of scales, at which DPDFs is computed, is given by $|\mathbf{y}^*|$:

$$\mathbf{y}^* = \begin{cases} \sim \mathbf{y} & \text{for } |\mathbf{y}| \ll y_{max} \\ \sim y_{max} & \text{for } |\mathbf{y}| \gtrsim y_{max} \end{cases} \quad (8)$$

- Matching should be computed at scales $\mu_{0i} \propto 1/|\mathbf{z}_i|$
→ evolve DPDFs to the matching scales using DGLAP equation.

Scales in the problem

- Rapidity dependence \rightarrow use the Collins-Soper equation for the matching kernels:

$$\frac{\partial}{\partial \log \sqrt{\zeta}} {}^{R_1 R'_1} C_{a_1 b_1}(x_1, \mathbf{z}_1; \mu_1, \zeta) = {}^{R_1} K_{a_1}(\mathbf{z}_1; \mu_1) {}^{R_1 R'_1} C_{a_1 b_1}(x_1, \mathbf{z}_1; \mu_1, \zeta). \quad (9)$$

${}^{R_1} K_{a_1}$ = colour factor \times singlet TMD Collins-Soper kernel.

Solution

$${}^{R_1 R'_1} C_{a_1 b_1}(x_1, \mathbf{z}_1; \mu_1, \zeta') = \exp\left({}^{R_1} K_{a_1}(\mathbf{z}_1; \mu_1) \log \frac{\sqrt{\zeta'}}{\sqrt{\zeta}}\right) {}^{R_1 R'_1} C_{a_1 b_1}(x_1, \mathbf{z}_1; \mu_1, \zeta). \quad (10)$$

Scales in the problem

Finally, matched DTMDs are evolved to the final scales $\sim Q_i$

Evolution equations for DTMDs

$$\begin{aligned}\frac{\partial}{\partial \log \sqrt{\zeta}} {}^{R_1 R_2} F_{a_1 a_2} &= \left[{}^{R_1} J(\mathbf{y}; \mu_i) + {}^{R_1} K(\mathbf{z}_1; \mu_1) + {}^{R_2} K(\mathbf{z}_2; \mu_2) \right] {}^{R_1 R_2} F_{a_1 a_2} , \\ \frac{\partial}{\partial \log \mu_1} {}^{R_1 R_2} F_{a_1 a_2} &= \left[\gamma_{a_1} - \gamma_{K, a_1} \log \frac{x_1 \sqrt{\zeta}}{\mu} \right] {}^{R_1 R_2} F_{a_1 a_2} .\end{aligned}\tag{11}$$

${}^1 J = 0$ at all orders!

Solution of the Collins-Soper equation for DTMDs

$$\begin{aligned} & R_1 R_2 F_{a_1 a_2}(x_i, \mathbf{z}_i, \mathbf{y}; \mu_{0i}, \zeta) \\ &= \exp\left(\left[R_1 J(\mathbf{y}; \mu_{0i}) + R_1 K(\mathbf{z}_1; \mu_{01}) + R_2 K(\mathbf{z}_2; \mu_{02})\right] \log \frac{\sqrt{\zeta}}{\sqrt{\zeta_0}}\right) R_1 R_2 F_{a_1 a_2}(x_i, \mathbf{z}_i, \mathbf{y}; \mu_{0i}, \zeta_0). \end{aligned} \quad (12)$$

Large- y behavior of the Collins-Soper kernel J – see [arXiv:2310.16432]

$${}^R J(\mathbf{y}; \mu_i) = {}^R J^{\text{pert.}}(\mathbf{y}^*; \mu_i) + \Delta {}^R J(\mathbf{y}), \quad \mathbf{y}^* - \text{regularized distance}, \quad (13)$$

$\Delta {}^8 J$ is $\mathcal{O}(-1)$ at large \mathbf{y} .

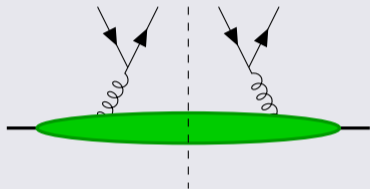
For large final scales one has a strong suppression of the color non-singlet channel at large \mathbf{y} .

Cross section in the large- y approximation

$$\frac{d\sigma_{DPS}}{\prod_{j=1,2} dx_j d\bar{x}_j d^2\mathbf{q}_j} = \frac{1}{1 + \delta_{A_1 A_2}} \sum_{a,b} \hat{\sigma}_{a_1 b_1} \hat{\sigma}_{a_2 b_2} \prod_{i=1,2} \int dz_i \frac{z_i}{2\pi} J_0(|\mathbf{q}_i| z_i) \\ \times \int_{y_{\text{cutoff}}}^{\infty} dy (2\pi y) \sum_R^{R_1 R_2} F_{a_1 a_2}^{\bar{R}_1 \bar{R}_2} F_{b_1 b_2} . \quad (14)$$

Initial conditions for collinear DPDs

Splitting part



Perturbative splitting at scale $\propto |\mathbf{y}^*|^{-1}$
 \times Gaussian to suppress at large \mathbf{y} .

Intrinsic part

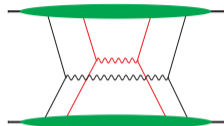
Product of PDFs \times further factors, see [Diehl, Gaunt, Lang, Plöb, Schäfer \[2001.10428\]](#).

$$R_1 R_2 F_{ab}^{intr.} = \text{colour factor}(R_1 R_2) \times {}^{11}F_{ab}^{intr.} . \quad (15)$$

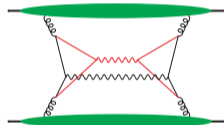
This form saturates the positivity bounds in colour space.

Combining the intrinsic and splitting parts

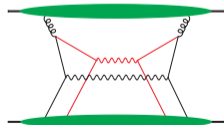
$$2\nu 2 \leftrightarrow F^{intr.} F^{intr.}$$



$$1\nu 1 \leftrightarrow F^{spl.} F^{spl.}$$



$$1\nu 2 \leftrightarrow F^{spl.} F^{intr.}$$



Numerical results – matched DTMDs in z -space

- ChiliPDF – C++ library for evolution and interpolation of parton distributions
Diehl, Nagar, Plößl, Tackmann [2305.0484]

Numerical results – matched DTMDs in z -space

- ChiliPDF – C++ library for evolution and interpolation of parton distributions
Diehl, Nagar, Plößl, Tackmann [2305.0484]
- Large distance Collins-Soper kernels as in Scimeni, Vladimirov [1912.06532]

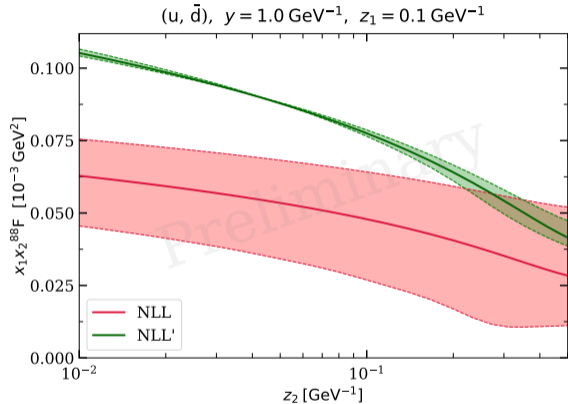
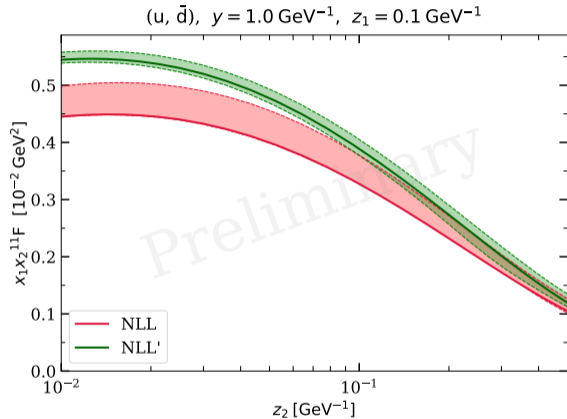
Numerical results – matched DTMDs in \mathbf{z} -space

- ChiliPDF – C++ library for evolution and interpolation of parton distributions
Diehl, Nagar, Plöb, Tackmann [2305.0484]
- Large distance Collins-Soper kernels as in Scimeni, Vladimirov [1912.06532]
- Hard scales $\mu_i = \sqrt{\zeta} = M_W$, $\sqrt{s} = 13$ TeV.
- $x_1 = x_2 = M_W/(13 \text{ TeV}) \approx 6 \times 10^{-3}$.
- $|\mathbf{z}_1| = 0.1 \text{ GeV}^{-1} = \text{const.}$

Numerical results – matched DTMDs in \mathbf{z} -space

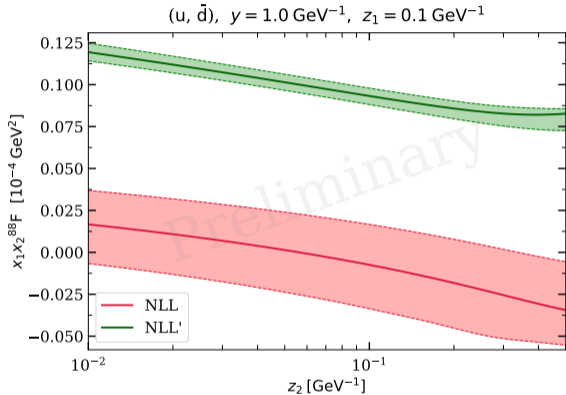
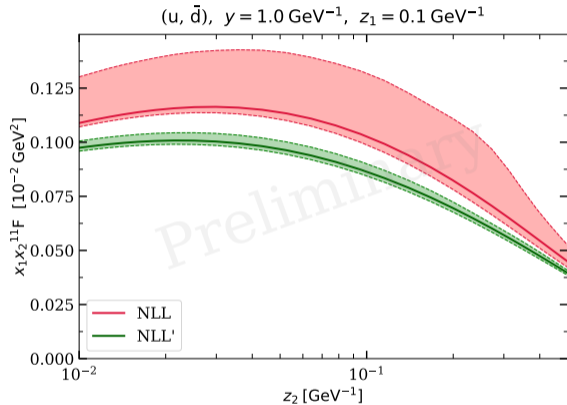
- ChLiPDF – C++ library for evolution and interpolation of parton distributions
Diehl, Nagar, Plöchl, Tackmann [2305.0484]
- Large distance Collins-Soper kernels as in Scimeni, Vladimirov [1912.06532]
- Hard scales $\mu_i = \sqrt{\zeta} = M_W$, $\sqrt{s} = 13$ TeV.
- $x_1 = x_2 = M_W/(13 \text{ TeV}) \approx 6 \times 10^{-3}$.
- $|\mathbf{z}_1| = 0.1 \text{ GeV}^{-1} = \text{const.}$
- Estimation of higher-order corrections
→ vary the matching scale from $\frac{1}{2} \frac{b_0}{|\mathbf{z}^*|}$ to $\frac{2b_0}{|\mathbf{z}^*|}$.

Numerical results – matched intrinsic DTMDs in z -space



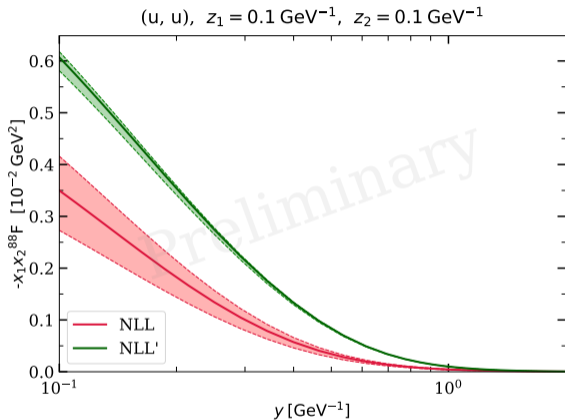
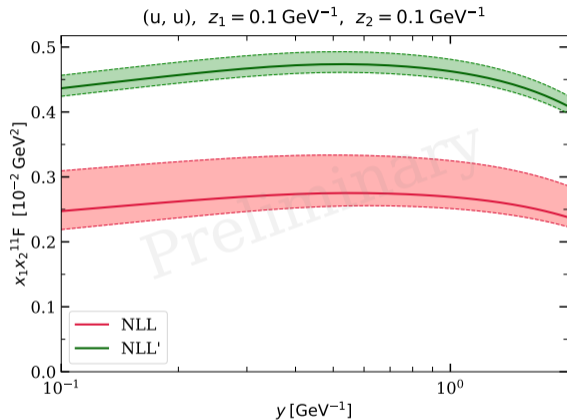
Unpolarized DTMDs matched onto intrinsic DPDFs. Left: singlet, right: colour octet. Bands represent the uncertainty estimation obtained by varying the matching scales.

Numerical results – matched intrinsic DTMDs in z -space



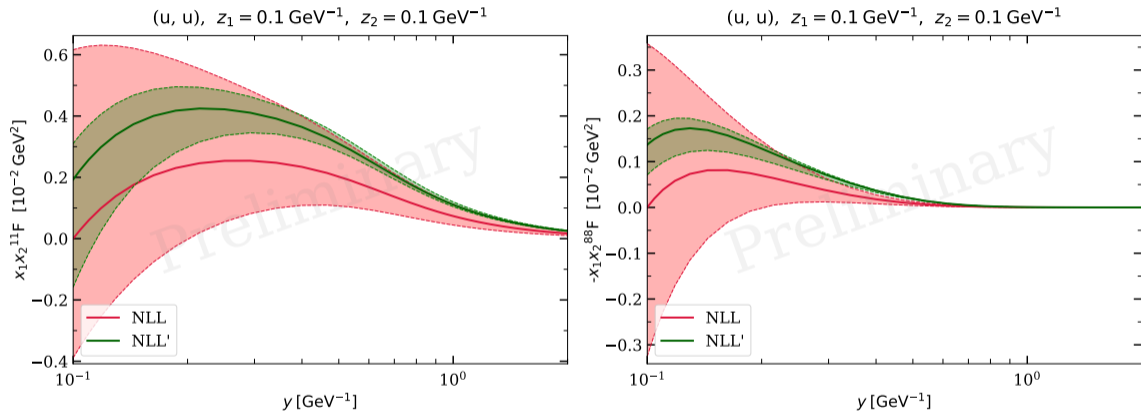
The same, but for longitudinally polarized quarks. Left: singlet, right: colour octet. Bands represent the uncertainty estimation obtained by varying the matching scales.

Numerical results – matched intrinsic DTMDs in y -space



Unpolarized DTMDs matched onto intrinsic DPDFs. Left: singlet, right: colour octet. Bands represent the uncertainty estimation obtained by varying the matching scales.

Numerical results – matched splitting DTMDs in y -space

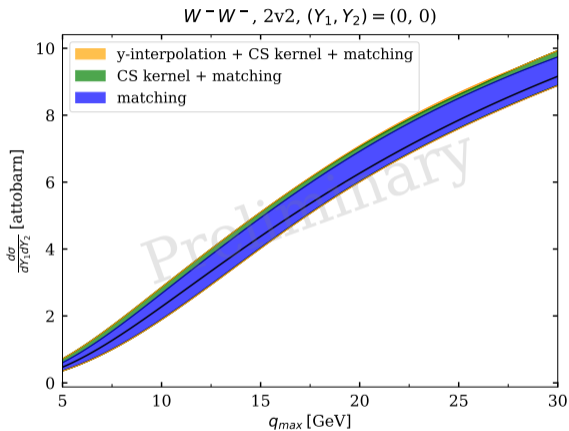
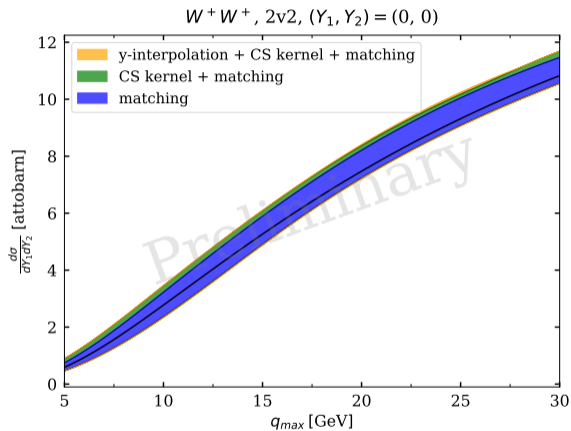


Unpolarized DTMDs matched onto intrinsic DPDFs. Left: singlet, right: colour octet. Bands represent the uncertainty estimation obtained by varying the matching scales.

Numerical results – cross section of $W^\pm W^\pm$ production

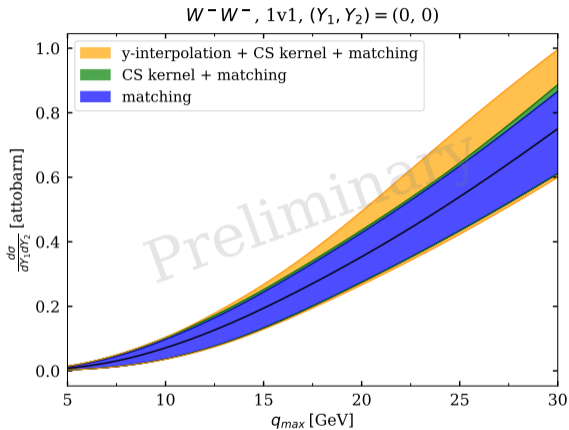
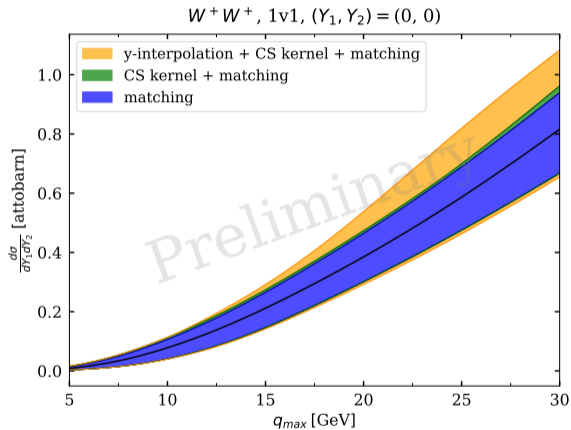
- Singlet contributions much larger than nonsinglet:
 - like-sign W : $\sigma^{\text{singlet}} \sim 10^3 \times \sigma^{\text{nonsinglet}}$.
 - opposite-sign W : $\sigma^{\text{singlet}} \sim 10^2 \times \sigma^{\text{nonsinglet}}$.
- For like-sign W pair cross section dominated by the intrinsic part:
 $\sigma^{\text{intr.}} \sim 10 \times \sigma^{1v2} \sim 20 \times \sigma^{\text{split}}$.
- Opposite-sign W : splitting and intrinsic terms give similar contributions.

Partially integrated cross-sections – 2v2



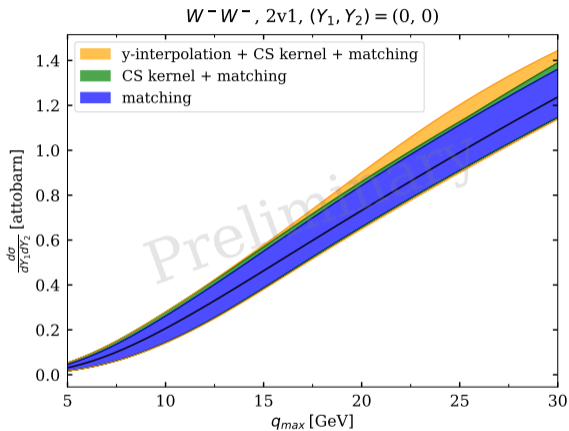
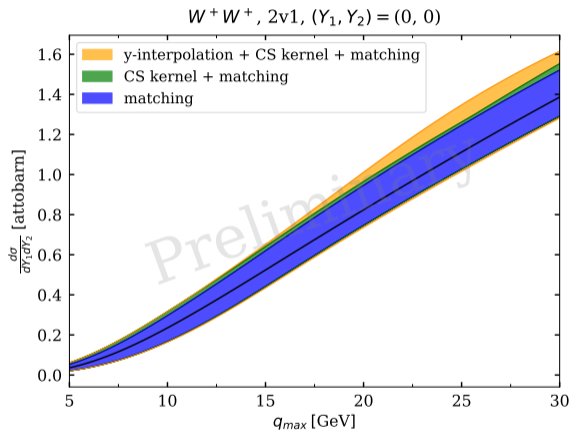
$$\frac{d\sigma^{DPS,2v2}}{\prod_{i=1,2} d\mathbf{q}_i dY_i} \text{ integrated over the transverse momenta } |\mathbf{q}| < q_{max}.$$

Partially integrated cross-sections – 1v1



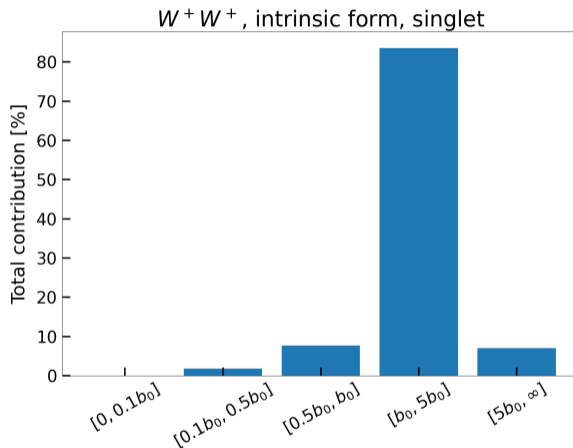
$$\frac{d\sigma^{DPS,1v1}}{\prod_{i=1,2} d\mathbf{q}_i dY_i} \text{ integrated over the transverse momenta } |\mathbf{q}| < q_{max}.$$

Partially integrated cross-sections – 2v1



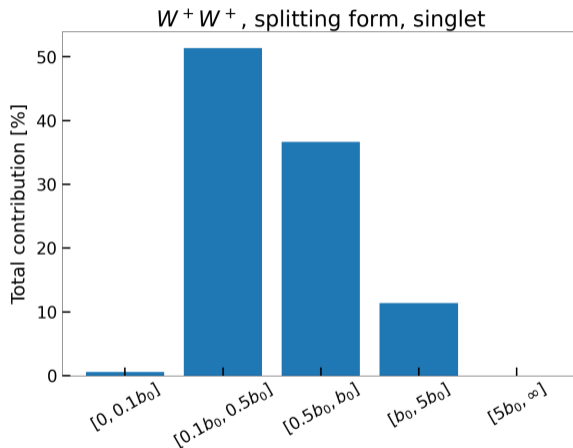
$$\frac{d\sigma^{DPS,2v1}}{\prod_{i=1,2} d\mathbf{q}_i dY_i} \text{ integrated over the transverse momenta } |\mathbf{q}| < q_{max}.$$

Contributions from different y -regions - intrinsic DPDFs.



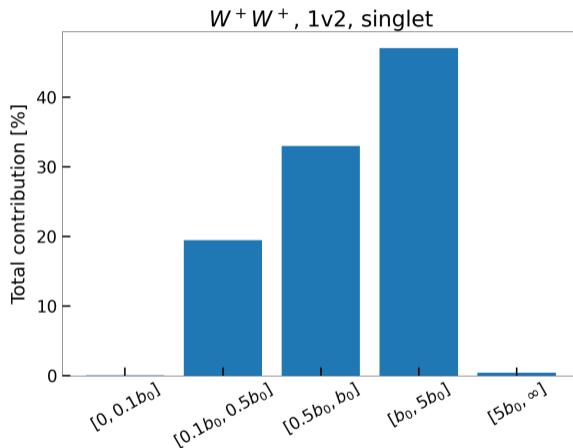
Contribution to differential cross section at zero rapidity integrated over q_T up to 20 GeV.

Contributions from different y -regions - splitting DPDFs.



Contribution to differential cross section at zero rapidity integrated over q_T up to 20 GeV.

Contributions from different y -regions - $1\nu 2$



Contribution to differential cross section at zero rapidity integrated over q_T up to 20 GeV.

Cross section in the short-distance approximation

DTMDs at initial scales expressed in terms of the splitting and intrinsic parts.

- Intrinsic part: $y = 0$ limit of DPDF intrinsic part.

Cross section in the short-distance approximation

DTMDs at initial scales expressed in terms of the splitting and intrinsic parts.

- Intrinsic part: $\mathbf{y} = 0$ limit of DPDF intrinsic part.
- Splitting part (known only at LO)

$$R_1 R_2 F_{a_1 a_2}^{spl.}(x_i, \mathbf{y}, \mathbf{z}_i; \mu_0) = \frac{\mathbf{y}_+^i \mathbf{y}_-^j}{\mathbf{y}_+^2 \mathbf{y}_-^2} \frac{\alpha_s(\mu_0)}{2\pi^2} R_1 R_2 T_{a_0 \rightarrow a_1 a_2}^{ij} \left(\frac{x_1}{x_1 + x_2} \right) \frac{f_{a_0}(x_1 + x_2)}{x_1 + x_2}, \quad (16)$$

$$\mathbf{y}_{\pm} = \mathbf{y} \pm \frac{1}{2}(\mathbf{z}_1 - \mathbf{z}_2). \quad (17)$$

Note: no LO splitting contribution for like-sign W production.

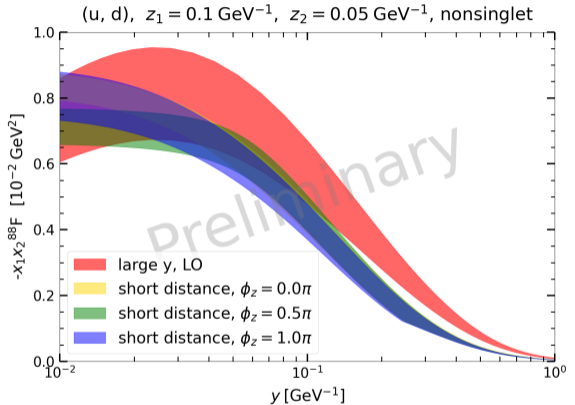
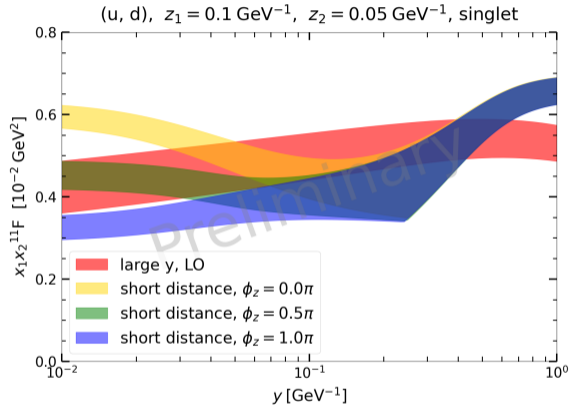
Only one initial scale (contrary to the large- y case), chosen as

$$\mu_0(\mathbf{y}, \mathbf{z}_1, \mathbf{z}_2) = b_0 / \sqrt{|\mathbf{y}_+^*| \times |\mathbf{y}_-^*|}. \quad (18)$$

Collins-Soper equation for DTMDs at small distances mixes color representations:

$$\begin{aligned} \frac{\partial}{\partial \log \zeta} {}^{R_1 R_2} F_{a_1 a_2}(x_i, y; \mu, \zeta) \\ = \frac{1}{2} {}^{R_1 R_2 R'_1 R'_2} K_{a_1 a_2}(\mathbf{y}, \mathbf{z}_i; \mu) {}^{R'_1 R'_2} F_{a_1 a_2}(x_i, y; \mu_i, \zeta) . \end{aligned} \quad (19)$$

Numerical results – short-distance vs large- y DTMDs in y -space.



Intrinsic DTMDs in two approximations. Left: singlet, right: colour octet. Presented are results for $\mathbf{y} \perp (\mathbf{z}_1 - \mathbf{z}_2)$ and different angles between \mathbf{z}_1 and \mathbf{z}_2 .

Cross section in the short-distance region

$\int d^2\mathbf{y} \sum_R R_1 R_2 F_{a_1 a_2}^{\bar{R}_1 \bar{R}_2} F_{b_1 b_2}$ depends on angle between \mathbf{z}_1 and \mathbf{z}_2
 \implies cannot reduce the Fourier transform to integrals with J_0 .

One can write

$$\int d^2\mathbf{y} \sum_R R_1 R_2 F_{a_1 a_2}^{\bar{R}_1 \bar{R}_2} F_{b_1 b_2} = \sum_{n=0}^{\infty} \cos(n\varphi_z) W_{a_1 a_2 b_1 b_2, n}(|\mathbf{z}_i|), \quad (20)$$

where φ_z is angle between \mathbf{z}_1 and \mathbf{z}_2 .

Cross section in the short-distance region

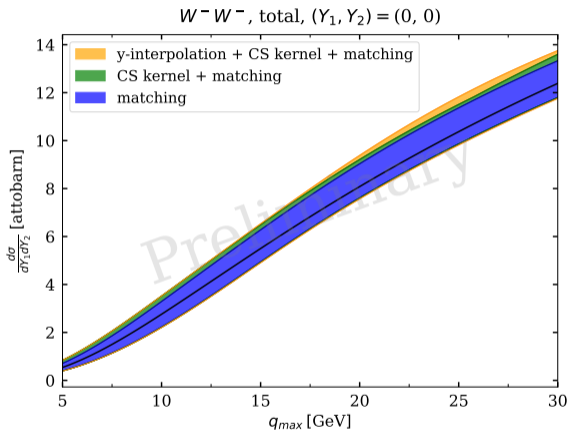
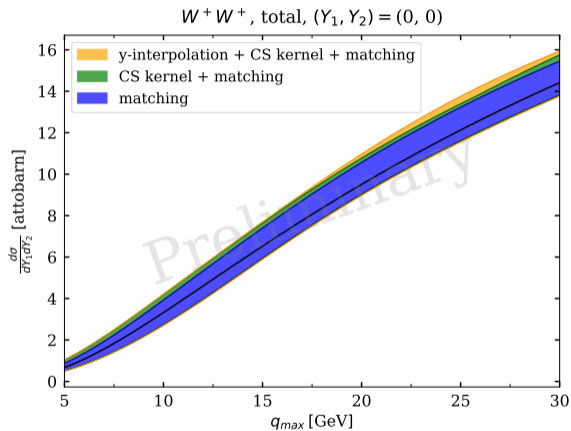
$$\frac{d\sigma_{DPS}}{\prod_{j=1,2} dx_i d\bar{x}_i d^2\mathbf{q}_i} = \frac{1}{1 + \delta_{A_1 A_2}} \sum_{a,b} \hat{\sigma}_{a_1 b_1} \hat{\sigma}_{a_2 b_2} \sum_{n=0}^{\infty} \cos(n\phi_q) \times \prod_{i=1,2} \int dz_i \frac{z_i}{2\pi} J_n(|\mathbf{q}_i| z_i) W_{a_1 a_2 b_1 b_2, n}(|\mathbf{z}_i|) . \quad (21)$$

ϕ_q - angle between \mathbf{q}_1 and \mathbf{q}_2 .

- Angular correlations between momenta of produced W bosons.
- Double Bessel integrals of different orders computed using Levin's method implemented in ChiliPDF.

D. Levin Fast integration of rapidly oscillatory functions, J. of Computational and Applied Mathematics 67 (1996) 95-101

Final results for like-sign W pairs production

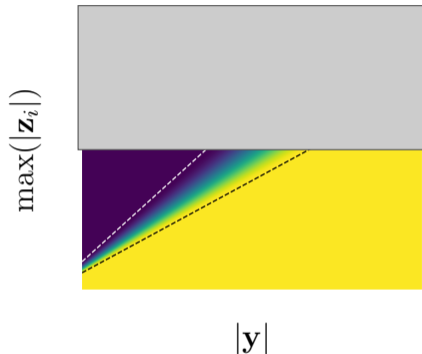


$$\frac{d\sigma^{DPS}}{\prod_{i=1,2} d\mathbf{q}_i dY_i} \text{ integrated over the transverse momenta } |\mathbf{q}| < q_{max}.$$

Summary

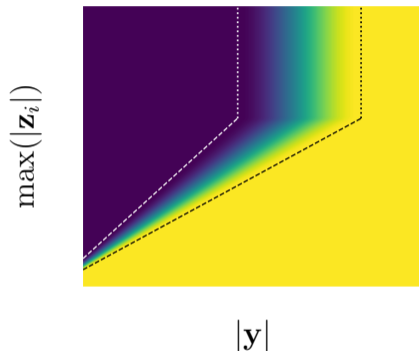
- Using the operator product expansion we obtain the description of DPS at large transverse momenta.
- Large- y approximation \rightarrow dominant contribution from the singlet intrinsic part in the region of nonperturbative y .
- Contribution from non-singlet DPDs to like-sign W production is strongly suppressed.
- Only the intrinsic part contributes to the short-distance part of like-sign W pair production cross section.
- Future work:
 - Computation of the short-distance contribution to W^+W^- production.
 - Study of uncertainties in the short-distance region.

Backup – interpolating between two regions



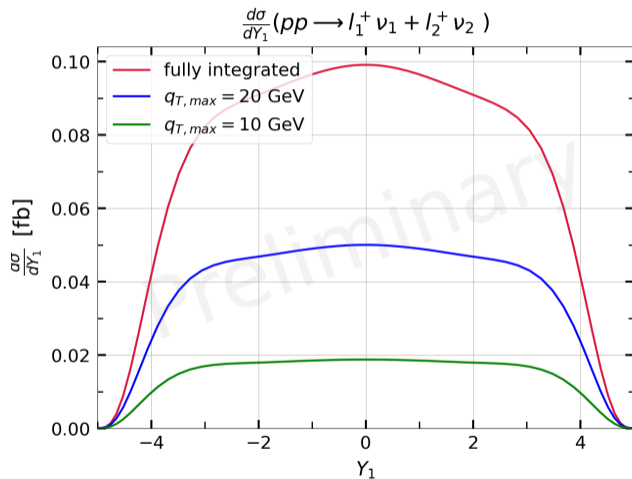
- Small z \rightarrow interpolate between two approximations in the overlap region.

Backup – extending the approximation to larger z

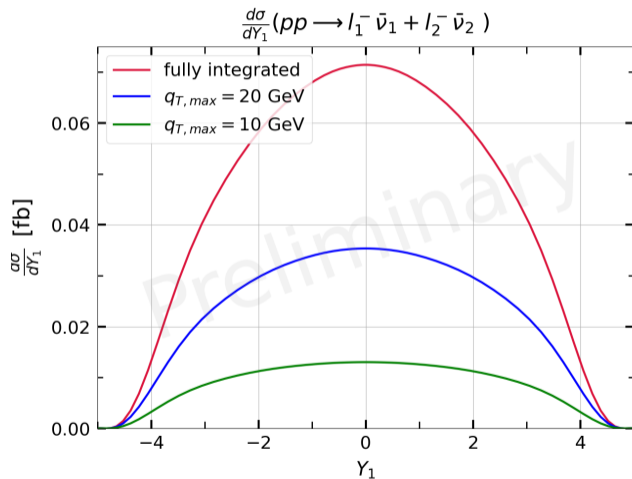


- Small $z \rightarrow$ interpolate between two approximations in the overlap region.
- $|y| > y_{\max} \implies$ match DTMD at regularized distances z^* , multiply by $e^{-\text{const.} \times z_i^2}$.
- At small y extrapolate the short-distance result. Interpolate for intermediate y .

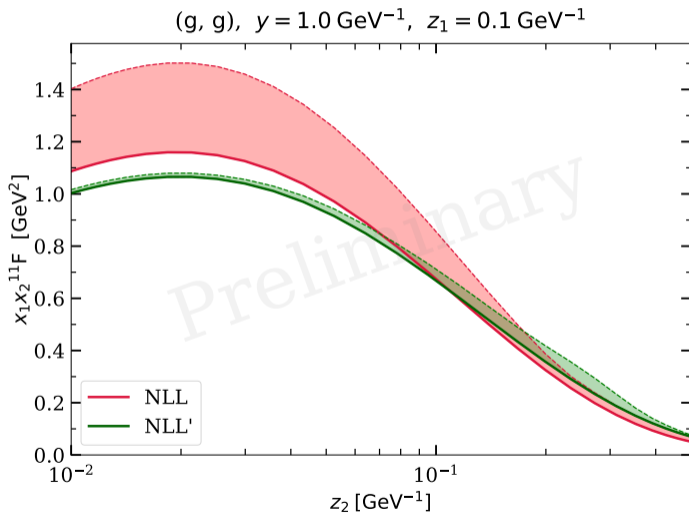
Backup – rapidity dependence for W^+W^+ .



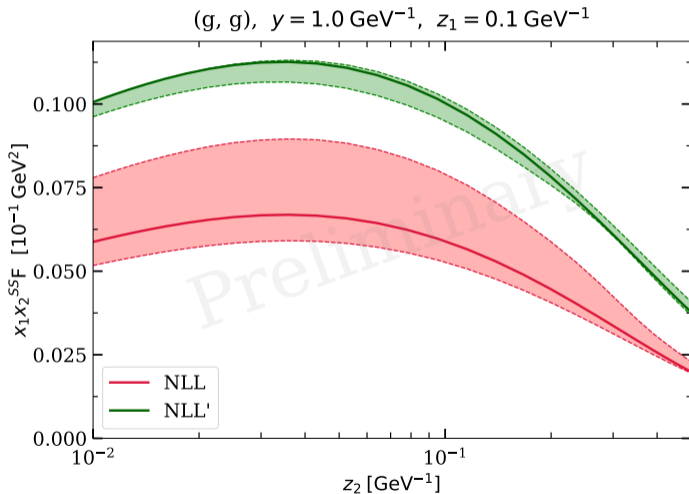
Backup – rapidity dependence for W^-W^- .



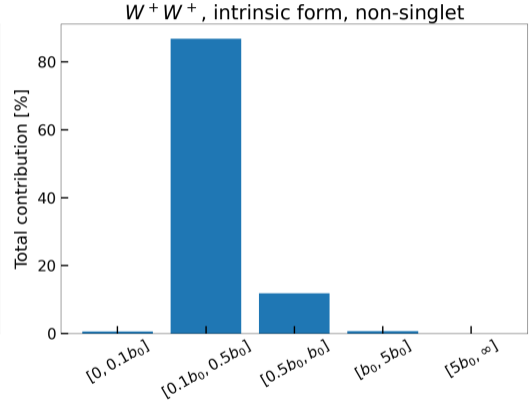
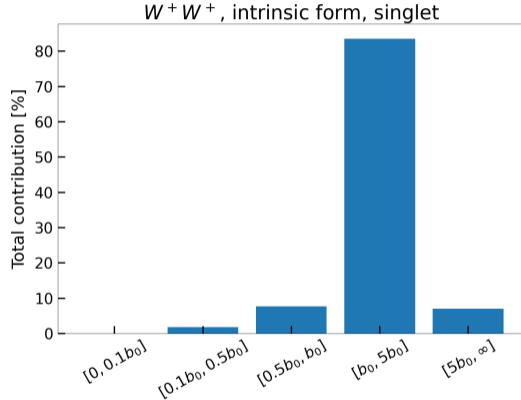
Backup – gluon DTMDs – $(R_1, R_2) = (1, 1)$



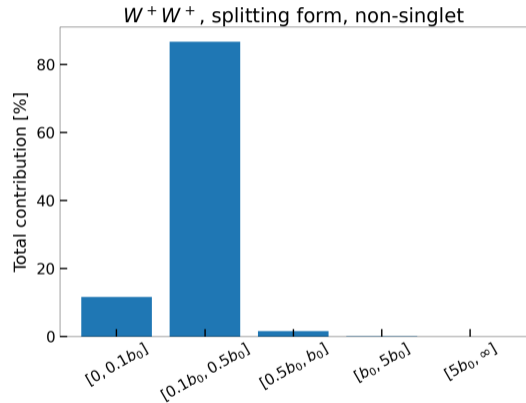
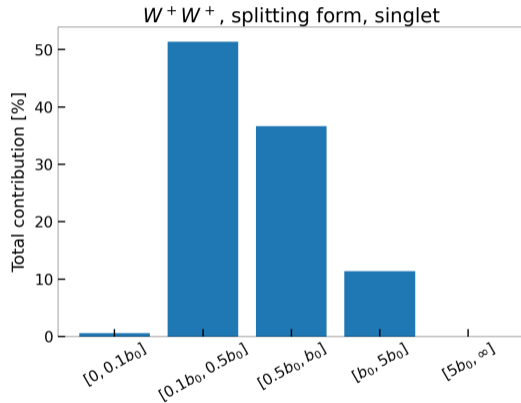
Backup – gluon DTMDs – $(R_1, R_2) = (S, S)$



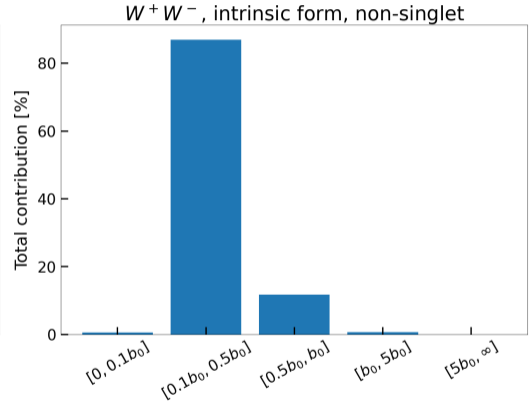
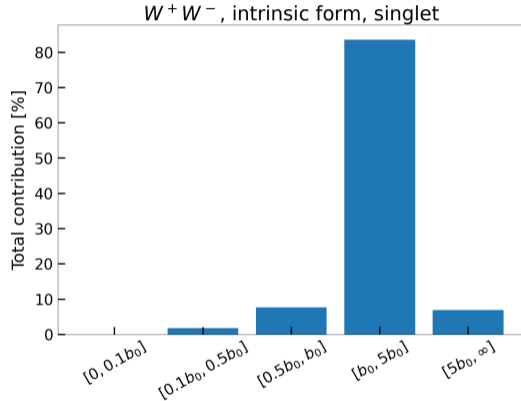
Backup – different y-regions for both color channels, intrinsic



Backup – different y-regions for both color channels, splitting



Backup – different y-regions for both color channels, opposite-sign W



Backup – different y-regions for both color channels, opposite-sign W

